

Lepton flavour-changing Scalar Interactions and Muon $g - 2$

Yu-Feng Zhou* and Yue-Liang Wu†

Institute of Theoretical Physics, Chinese Academy of Science, Beijing 100080, China

(Dated: February 8, 2020)

Abstract

A systematic investigation on muon anomalous magnetic moment and related lepton flavour-violating process such as $\mu \rightarrow e\gamma$, $\tau \rightarrow e\gamma$ and $\tau \rightarrow \mu\gamma$ is made at the two loop level in the models with flavour-changing scalar interactions. The two loop diagrams with double scalar exchanges are studied and their contributions are found to be compatible with the ones from Barr-Zee diagram. By comparing with the current data, the allowed ranges for the relevant Yukawa couplings Y_{ij} in lepton sector are obtained. The results show a hierarchical structure of $Y_{\mu e, \tau e} \ll Y_{\mu\tau} \simeq Y_{\mu\mu}$ in the physical basis, which deviates from the widely used ansatz in which the off diagonal elements are proportional to the square root of the products of related fermion masses. An alternative Yukawa coupling matrix in the lepton sector is suggested to understand the current data. With such a reasonable Yukawa coupling ansatz, the decay rate of $\tau \rightarrow \mu\gamma$ is found to be near the current experiment upper bound.

PACS numbers: 12.60.Fr, 13.40.Em, 13.35.-r

arXiv:hep-ph/0110302v2 31 Oct 2001

*Email: zhouyf@itp.ac.cn

†Email: ylwu@itp.ac.cn

Recently, the Muon $g - 2$ Collaboration at BNL reported their improved result on the measurement of muon anomalous magnetic moment ($g - 2$) [1]. The difference between the measurement and the Standard Model (SM) prediction [2] is reported as follows

$$\Delta a_\mu = a_\mu^{\text{exp}} - a_\mu^{\text{SM}} = (426 \pm 165) \times 10^{-11}, \quad (1)$$

which shows a large deviation ($\sim 2.6\sigma$) from the SM prediction. At 90% confidence level, Δa_μ lies in the range

$$113 \times 10^{-11} \leq \Delta a_\mu \leq 749 \times 10^{-11}. \quad (2)$$

Although this result implies the existence of new physics beyond the SM, it also imposes strong constraints on new physics models. Recently, large amount of work has been done in checking the new physics contributions to muon $g - 2$ by using model dependent[3, 4] and independent approaches [5].

In this paper, we would like to focus on a general discussion on the models with lepton flavor-changing scalar interactions where the new physics contributions mainly arise from Yukawa couplings. Such models may be considered as the simple extension of the standard model (SM) with more than one Higgs doublet ϕ_i ($i > 1$) but without imposing any discrete symmetry. The simplest one is the extension of SM with two Higgs doublets (S2HDM)[6] motivated from the spontaneous CP violation[7, 8]. In general, each Higgs doublet could receive vacuum expectation values (VEVs), but one can always rotate to a convenient basis so that only one of them has the VEV $v = (\sum_i v_i^2)^{1/2} = (\sqrt{2}G_F)^{-1/2} = 246$ GeV. Such a Higgs doublet will play the same role as the one in the SM. In such a basis, the interactions related to the remaining scalars represent the new physics effects beyond the SM.

The general form of Yukawa interaction is given by

$$\mathcal{L}_Y = \bar{\psi}_L^i Y_{ij}^a \psi_R^j \phi_a, \quad (3)$$

where Y_{ij}^a ($i, j = 1, 2, 3$) is the Yukawa coupling matrices. The index $a = 1, 2, \dots$ labels the Higgs doublets. The behavior of the Yukawa interactions depends on the texture of Yukawa coupling matrices. In general there are two kind of assumptions on Yukawa coupling matrices in mass eigenstates:

1. Yukawa coupling matrices of the scalar interactions are diagonal.
2. Yukawa coupling matrices of the scalar interactions contain non-zero off-diagonal elements

The first ansatz is often used to avoid the flavour-changing neutral current (FCNC) at tree level which was originally suggested from the kaon physics, such as $K \rightarrow \mu^+ \mu^-$ decay and $K^0 - \bar{K}^0$ mixing. Such a texture structure of the Yukawa couplings can be obtained by imposing some kind of discrete symmetries[9]. The minimal SUSY Standard Model (MSSM) and the two-Higgs-doublet model (2HDM) of type **I** and **II** can be cataloged into this type. In such models, the Yukawa interactions are flavour conserving and the couplings are proportional to the related fermion masses

$$Y_{ii} = \frac{gm_i}{2m_W} \xi_i \quad \text{and} \quad Y_{ij} = 0. \quad (4)$$

where g is the weak coupling constant and m_W is the mass of W boson. ξ_i is the rescaled coupling constant. In the minimal SUSY model and the 2HDM of type **II**, $\xi_i = \tan \beta (\cot \beta)$

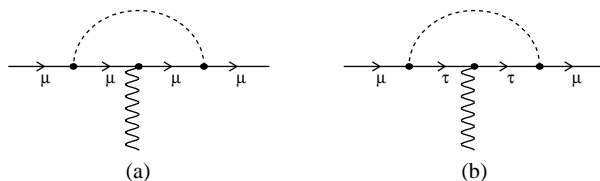


FIG. 1: One loop diagram contribution to muon $g - 2$. The dashed curves represent the scalar or pseudo-scalar propagator. (a) Flavour conserving Yukawa interactions. (b) Flavour changing Yukawa interactions in which μ changes into τ or e in the loop. The main contribution from internal τ loop

for down (up) type fermions. The corresponding contributions to muon $g - 2$ at one loop level which is shown in Fig.1 have been recently discussed and compared with the current data in Ref.[10, 11, 12].

As the muon lepton mass is small, i.e., $m_\mu \ll m_\phi$, where m_ϕ is the mass of scalar ($\phi = h$) or pseudo-scalar ($\phi = A$), the one loop contribution to muon $g - 2$ can be written as [13]

$$\Delta a_\mu = \pm \frac{1}{8\pi^2} \frac{m_\mu^2}{m_\phi^2} \ln \left(\frac{m_\phi^2}{m_\mu^2} \right) Y_{ii}^2 \quad (5)$$

where the sign “+ (-)” is for scalar ($\phi = h$) (pseudo-scalar $\phi = A$) exchanges. It can be seen from the above equation that the one loop scalar contribution is not large enough to explain the current data. Even for a large value of $\xi_\mu = \tan \beta \sim 50$, one still needs a very light mass of the scalar $M_h \sim 5$ GeV, which seems not favored by the LEP experiment. The situation will be even worse when both the scalar and pseudo-scalar are included as their contributions have opposite signs.

It will be quite different if one goes to two loop level. From the well known Barr-Zee mechanism[14] (see. Fig.2a)in which the scalar or pseudo-scalar couples to a heavy fermion loop. As the Yukawa couplings are no longer suppressed by the light fermion mass, the two loop contributions could be considerable. Taking the top quark loop as an example, the two

loop Barr-Zee diagram contribution to muon $g - 2$ is given by

$$\Delta a_\mu^h = \frac{N_c q_t^2 m_\mu m_t}{\pi^2 m_\phi^2} F\left(\frac{m_t^2}{m_\phi^2}\right) Y_{tt} Y_{\mu\mu} \quad (6)$$

where $N_c = 3$ and $q_t = 2/3$ are the color number and the charge of top quark respectively. The integral function $F(z)$ has the following form

$$F(z) = \begin{cases} -\frac{1}{2} \int_0^1 dx \frac{1-2x(1-x)}{x(1-x)-z} \ln \frac{x(1-x)}{z} & \text{for scalar} \\ \frac{1}{2} \int_0^1 dx \frac{1}{x(1-x)-z} \ln \frac{x(1-x)}{z} & \text{for pseudo-scalar} \end{cases} \quad (7)$$

The numerical calculation of Barr-Zee diagram contribution to muon $g - 2$ is shown in Fig.3

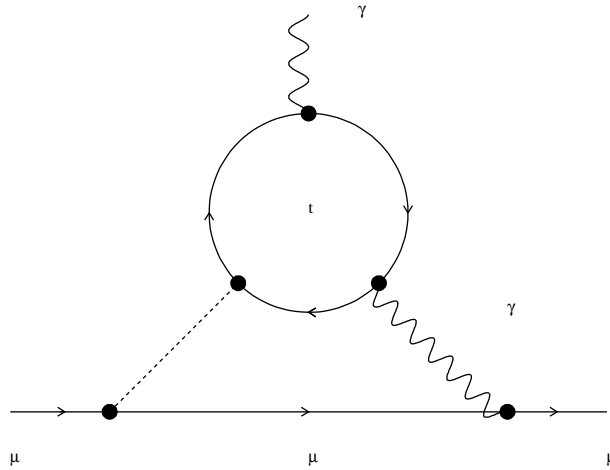


FIG. 2: Two loop Barr-Zee diagram contribution to muon $g - 2$.

It is noticed that the contributions from Barr-Zee diagram through scalar and pseudo-scalar exchanges have also different sign, negative for scalar and positive for pseudo-scalar, which is just opposite to the one loop case. Thus there exists a cancelation between one and two loop diagram contributions. It was found in Refs.[15, 16] that the pseudo-scalar exchanging Barr-Zee diagram can overwhelm its negative one loop contributions and results in a positive contribution to $g - 2$. For a sufficient large value of the coupling $\xi_\mu = \tan \beta \sim 50$, its contribution can reach the experimental bound with $m_\phi \leq 70\text{GeV}$. To avoid the cancelation between scalar and pseudo-scalar exchange, the mass of the scalar boson has to be pushed to be very heavy (typically greater than 500 GeV).

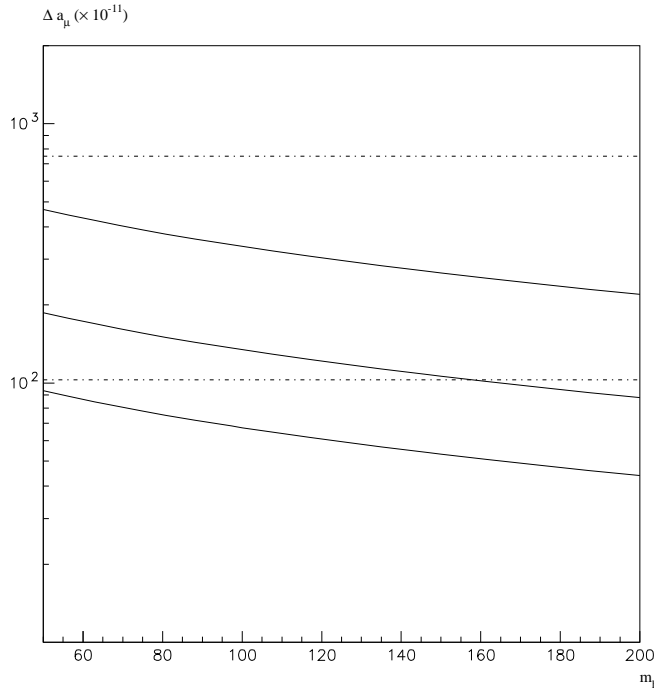


FIG. 3: Contribution to muon $g - 2$ from the two loop Barr-Zee diagrams. The three solid curves (from down to up) correspond to $Y_{\mu\mu} = 2 \times 10^{-2}, 4 \times 10^{-2}$ and 1×10^{-1} respectively. The two horizontal lines represent the allowed rang of muon $g - 2$ at 95%CL.

The above conclusion is obtained in the condition that the Yukawa couplings Y_{ij} are real. As it is noticed in our recent paper[4] that Y_{ij} may be complex in the most general case. In such a case, the scalar and pseudo-scalar are mixed together and the interference between one loop and two loop Barr-Zee diagram is not always destructive. In a large parameter space the interference could be constructive, and the allowed ranges for the couplings and the scalar (pseudo-scalar) mass become wider.

When imposing the strict discrete symmetries to Yukawa interaction, the off-diagonal elements of Yukawa coupling matrix are all zero. This is the simplest way to prevent the theory from tree level FCNC. However, to meet the constraints from the data on $K^0 - \bar{K}^0$ mixing and $K \rightarrow \mu^+ \mu^-$ the off-diagonal elements do not necessarily to be zero. An alternative way is to impose some approximate symmetries such as global family symmetry [6] on the Lagrangian. This results in the second ansatz of the Yukawa matrices in which small off-diagonal matrix elements are allowed. This leads to an enhancement for many flavour changing processes. As the constraints from $K^0 - \bar{K}^0$ mixing are strong, the corresponding off-diagonal matrix elements should be very small. However, up to now there is no such strong experimental constraints on the FCNC processes involving heavier flavors. The off-diagonal elements associated with the second and the third generation fermions are allowed to be larger. One of the widely used ansatz of the Yukawa matrix basing on the hierarchical fermion mass spectrum $m_{u,d} \ll m_{c,s} \ll m_{t,b}$ was proposed by Cheng and Sher [17, 18]. In

this ansatz, the off-diagonal matrix element has the following form:

$$Y_{ij} = \frac{g\sqrt{m_i m_j}}{2m_W} \xi_{ij} \quad (8)$$

where ξ_{ij} s are the rescaled Yukawa couplings which are roughly of the same order of magnitudes for all i, j s. In this ansatz, the scalar or pseudo-scalar mediated $d - s$ transition is strongly suppressed by small factor $\sqrt{m_d m_s}/(2m_W) \simeq 4 \times 10^{-4}$, which easily satisfied the constraints from $\Delta m_K, \epsilon_K$ and $\Gamma(K \rightarrow \mu^+ \mu^-)$. As the couplings grow larger for heavier fermions, the tree level FCNC processes may give considerable contributions in $B^0 - \bar{B}^0$ mixing, $\mu^+ \mu^- \rightarrow tc, \mu\tau$ and several rare B and τ decay modes. [19, 20, 21, 22].

Unlike the flavour-conserving one loop diagrams, the flavour-changing one loop diagrams with internal heavy fermions can give large contribution to muon $g - 2$. The reason is that the loop integration yield an enhancement factor of $\sim m_i \ln(m_i^2/m_\phi^2)/(m_\mu \ln(m_\mu^2/m_\phi^2))$. For the internal τ loop, it is a factor of $\mathcal{O}(10)$. If one uses the scaled coupling $\xi_{\mu\tau}$ and takes $\xi_{\mu\tau} \simeq \xi_{\mu\mu}$ as in the ‘‘Cheng-Sher’’ ansatz, the value of the enhancement factor can reach $\mathcal{O}(10^2)$. In the following discussion, for simplicity we only take one loop diagram with internal τ loop into consideration as it is dominated over other fermion loops in the case that the Yukawa couplings are of the same order of magnitudes.

The expression of one loop flavor changing diagram contribution to muon $g - 2$ is given by [23]

$$\begin{aligned} \Delta a_\mu &= \pm \frac{1}{8\pi^2} \frac{m_\mu m_\tau}{m_\phi^2} \left(\ln \frac{m_\phi^2}{m_\tau^2} - \frac{3}{2} \right) Y_{\mu\tau}^2 \\ &= \pm \frac{g^2}{32\pi^2} \frac{m_\mu^2 m_\tau^2}{m_W^2 m_\phi^2} \left(\ln \frac{m_\phi^2}{m_\tau^2} - \frac{3}{2} \right) \xi_{\mu\tau}^2 \end{aligned} \quad (9)$$

where the sign ‘‘+ (-)’’ is for scalar ($\phi = h$) (pseudo-scalar $\phi = A$) exchanges. For detailed discussion on one loop flavour changing diagram, we refer to the Refs.[24, 25].

As the two loop contribution to muon $g - 2$ is more considerable via the Barr-Zee mechanism in flavor-conserving case, it is nature to go further to consider the same diagram with flavour-changing couplings. However, in the case of muon $g-2$, as the initial and final states are all muons, it is easy to see that the Barr-Zee diagram with flavor-changing coupling can not contribute. It can only appear in flavor changing process such as $\mu \rightarrow e\gamma$. The non-trivial two loop diagrams which give non-negligible contribution to $g-2$ are those diagrams (as shown in Fig.10) which have two internal scalars with both of them coupling to a heavy fermion loop.

It is known that large Yukawa couplings between scalar and heavy fermions can compensate the loop suppressing factor $g^2/16\pi^2$ and make the Barr-Zee diagram to be sizable. The same mechanism also enhances the two-loop double scalar exchanging diagrams. Further more, in the flavour changing case, the μ lepton can go into heavier lepton τ in the lower loop, this may provide an additional enhancement in loop integration. Taking the internal t -quark loop as an example, the ratio between the contribution to muon $g - 2$ from two-loop double scalar diagrams relative to the one from Barr-Zee type diagrams can be roughly estimated by the ratio between the couplings, which gives $\sim \xi_t \xi_{\mu\tau}^2 m_t m_\tau / (4\xi_\mu m_W^2 \sin^2 \theta_W)$, where θ_W is Weinberg angle with the value $\sin^2 \theta_W \simeq 0.23$. For the typical values of $\xi_t = 1$ and $\xi_{\mu\tau} \simeq \xi_\mu = 30$ the ratio is of order 1. Thus this kind of two-loop double scalar-exchanging

diagram is compatible with the one of Barr-Zee type. In the large m_t limit, the contribution to muon $g - 2$ from two loop double scalar (pseudo-scalar) exchanging diagram can be written as follows

$$\Delta a_\mu = \mp \frac{N_C g^4 m_\tau m_\mu m_f^2}{16\pi^4 m_\phi^4} \left(-\frac{5}{2} + \ln \frac{m_\phi^2}{m_\tau^2} \right) Y_{tt}^2 Y_{\mu\tau}^2 \quad (10)$$

The details of the two loop calculations can be found in the appendix at the end of this paper. Comparing with the one-loop flavour-changing diagram in the same way, one can see that this diagram is quite sizable. The numerical results are shown in Fig.4 and Fig.5.

For a comparison, the contribution to muon $g - 2$ from two-loop double pseudo scalar-exchanging diagrams and Barr-Zee diagrams with pseudo-scalar are shown in Fig.4.

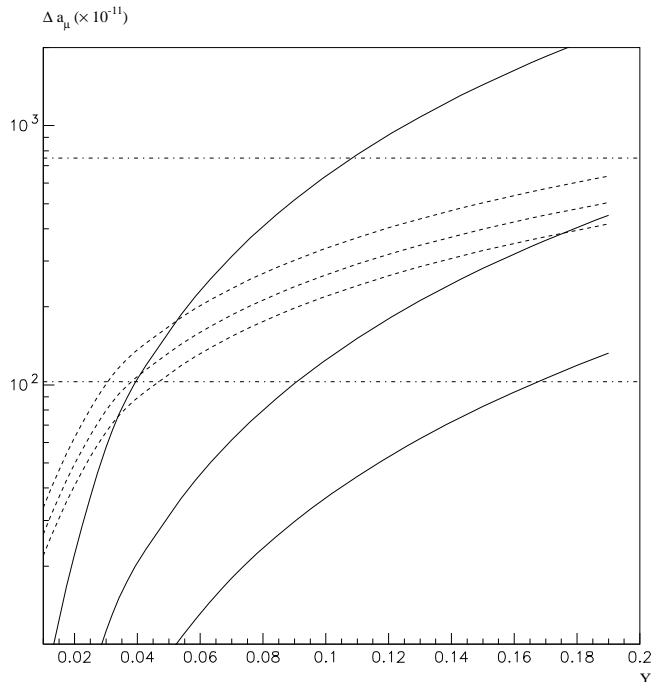


FIG. 4: Comparison between two loop Barr-Zee pseudo-scalar and double pseudo-scalar exchanging diagram in contribution to muon $g - 2$. The contribution to muon $g - 2$ is plotted as function of $Y = Y_{\mu\tau} = Y_{\mu\mu}$. Three solid curves (from up to down) correspond to double scalar exchanging diagram contribution with scalar (pseudo-scalar) mass $m_{h(A)} = 100, 150, 200$ respectively. Three dashed curves indicate the one from two loop Barr-Zee diagrams with pseudo-scalar exchange. The two horizontal lines represent the allowed range of $g - 2$ at 95%CL.

To make the two kind of contributions comparable, we take $Y_{\mu\mu} = Y_{\mu\tau} \equiv Y$. It can be seen that the contribution from the former highly depends on the coupling Y and the scalar mass. In the range $0.05 \leq Y \leq 0.15$, the contribution from double scalar-exchanging diagram is much large than the one from Barr-Zee diagram when $m_{h(A)}$ is about $100 \sim 150$ GeV. it decrease with $m_{h(A)}$ increasing and becomes quite small when $m_{h(A)} \sim 200$ GeV. In Fig.5, the

contribution to muon $g - 2$ from two-loop double scalar-exchanging diagrams is compared with the one from the corresponding flavour-changing one loop diagrams. Note that just like the case of Barr-Zee diagram, the two-loop double scalar-(pseudo-scalar) exchanging diagrams give negative (positive) contributions, which have the opposite signs as the one from one loop scalar (pseudo-scalar)- exchanging diagram. This results in a strong cancelation between one and two loop diagram contributions in the case of flavour changing couplings with real Yukawa coupling constants. The allowed range of the scalar mass will be strongly constrained. Taking $Y_{\mu\tau} = 0.08(\xi_{\mu\tau} \simeq 50)$ and $Y_{tt} = 0.67(\xi_t \simeq 1)$ as an example, the mass of scalar m_h lies in a narrow window of $\sim 100 \leq m_h \leq 200$ GeV.

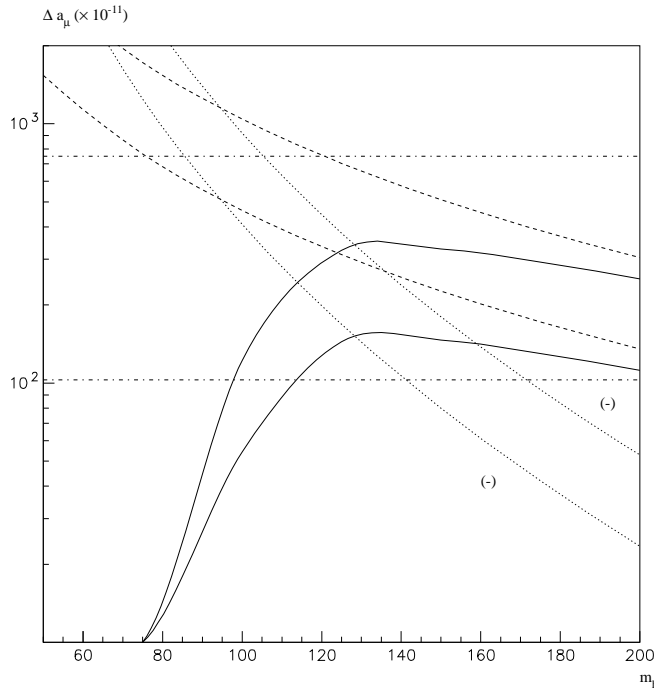


FIG. 5: Comparison between one loop and two loop double scalar exchange diagrams in contribution to muon $g - 2$. The contribution to muon $g - 2$ is plotted as function of scalar mass. The two dashed curves represent the contribution at one loop with $Y_{\mu\tau}=0.12$ (up) and 0.08 (down) respectively. The two dotted curves correspond to the one from two loop double scalar diagram with the same couplings. (Note that their contribution are negative) The solid curves are the total contribution to $g - 2$ from the both diagrams. The two horizontal lines represent the allowed rang of $g - 2$ at 95%CL.

As it is mentioned in the above discussion, the constraints may be weaker if the Yukawa couplings Y_{ij} are allowed to be complex. In this case the couplings in Eq.(6) and Eq.(10) should be replaced as

$$\begin{aligned} Y_{tt}Y_{\mu\mu} &\rightarrow |Y_{tt}Y_{\mu\mu}| \cos \delta_t \cos \delta_{\mu\mu} \\ Y_{tt}^2 Y_{\mu\tau}^2 &\rightarrow |Y_{tt}Y_{\mu\tau}|^2 \cos 2\delta_t \cos 2\delta_{\mu\tau} \end{aligned} \quad (11)$$

respectively, with δ_t and $\delta_{\mu\tau}$ being the phases of the corresponding couplings. Although the one and two loop share the same phase in the coupling $Y_{\mu\tau}$ or $Y_{\mu\mu}$, the non-zero phase of δ_f

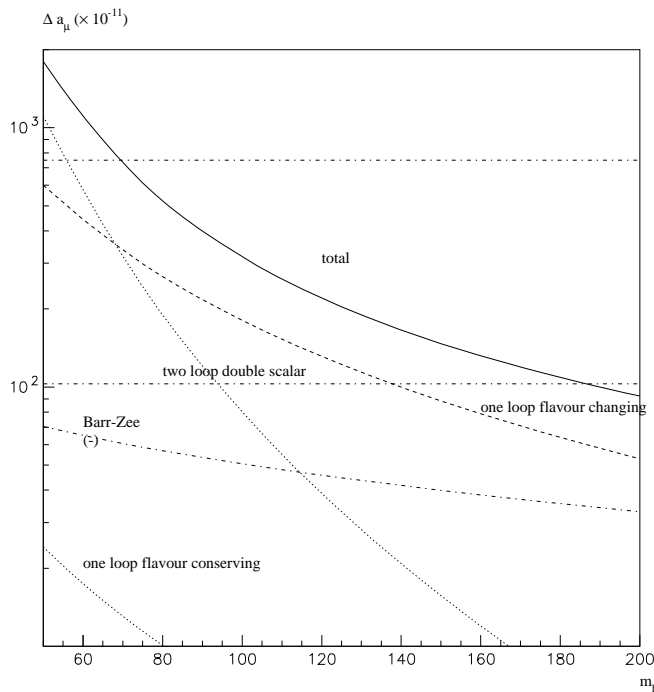


FIG. 6: Total contribution to muon $g - 2$ in the case of non-zero phases, with $Y_{\mu\tau} = 0.05$, $Y_{\mu\mu} = 0.03$, $\delta_t = 2\pi/3$ and $\delta_{\mu\tau} = \delta_{\mu\mu} = 0$. The curves correspond to the contributions from one loop flavour changing, one loop flavour conserving, two loop double scalar exchanging and two loop Barr-Zee diagrams (which is negative) respectively. The two horizontal lines represent the allowed range of $g - 2$ at 95%CL.

may change the interference between one and two loop diagrams. a small value of $\cos 2\delta_f$ may reduce the contribution from two loop double scalar diagrams or turn their signs to be positive. Taking $\delta_t = 2\pi/3$ as an example, we show in Fig.6 that in this case the total contribution to muon $g - 2$ would be large enough to meet the current data with reasonable values of the couplings $Y_{\mu\tau}$ and $Y_{\mu\mu}$.

The flavor changing Yukawa couplings will unavoidably lead to the enhancement of decay rates of lepton flavor violating processes. such as $\mu \rightarrow e\gamma$, $\tau \rightarrow \mu(e)\gamma$, $\mu \rightarrow e^-e^-e^+$ and $\tau \rightarrow e^-e^-e^+(\mu^-\mu^-\mu^+)$. The current experimental data especially the data of $\mu \rightarrow e\gamma$ will impose strongest constraints on the related Yukawa couplings. From the current data the upper bound of the decay $\mu \rightarrow e\gamma$ is $\Gamma(\mu \rightarrow e\gamma) \leq 3.6 \times 10^{-30}$ GeV [26]. It constrains the coupling $Y_{e\tau(\mu)}$ to be extremely small. In the models with flavour changing scalar interactions, The leading contributions to $\mu \rightarrow e\gamma$ come from the one loop flavour changing diagram, the two loop double scalar exchanging diagram and the two loop flavour changing Barr-Zee diagrams. In Fig.7 the sum of the first two diagrams are presented as function of the scalar mass. In the calculation we take the value of coupling $Y_{tt} = 0.67$ (or $\xi_t \simeq 1$). The value of $Y_{\mu\tau}$ is taken to be 0.08 (or $\xi_{\mu\tau} \simeq 50$) which is the typical allowed value from the current data on $g - 2$. It can be seen from the figure that the decay rate of $\mu \rightarrow e\gamma$ constrain the value of $Y_{\tau e}$ to be no more than $10^{-6} \sim 10^{-5}$ for $100 \leq m_h \leq 200$ GeV.

Similarly, the value of coupling $Y_{\mu e}$ is also constrained to be very small by the decay rate

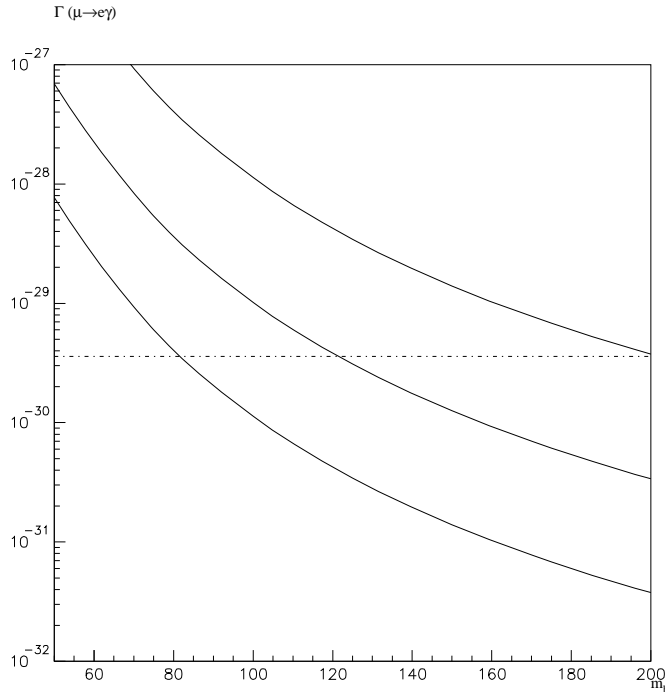


FIG. 7: Contribution to decay $\mu \rightarrow e\gamma$ from the sum of one loop and two loop double scalar diagrams. The three solid curves (from down to up) correspond to $Y_{\tau e} = 1 \times 10^{-6}, 3 \times 10^{-6}$ and 1×10^{-5} respectively. The coupling $Y_{\mu\tau}$ is taken to be 0.08. The horizontal line indicates the experimental upper bound of $\mu \rightarrow e\gamma$

$\mu \rightarrow e\gamma$. The reason is that $Y_{\mu e}$ is associated with the flavour changing Barr-Zee diagram in which muon goes into tau in the lower loop. If there is no accidental cancelation with other diagrams the upper bound of $Y_{\mu e}$ can be obtained by assuming that the flavour changing Barr-Zee diagram is dominant. The result is shown in Fig. 8, the upper bound of $Y_{\mu e}$ is also of the order $10^{-6} \sim 10^{-5}$ for $100 \leq m_h \leq 200\text{GeV}$.

With the above constraints on the values of Yukawa couplings in the lepton sector, let us discuss the possible texture of Yukawa coupling matrix. In the SM with one Higgs doublet, it is well known that by assuming the Yukawa matrix to be of the Fritzsch form [27] in flavour basis, i.e.

$$Y \simeq \begin{pmatrix} 0 & \sqrt{m_1 m_2} & 0 \\ \sqrt{m_1 m_2} & 0 & \sqrt{m_2 m_3} \\ 0 & \sqrt{m_2 m_3} & m_3 \end{pmatrix} \quad (12)$$

one can reproduce not only correct quark masses in mass eigenstates but also, in a good approximation, some of the CKM matrix elements. In the models with multi-Higgs doublets, one can simply extend this Fritzsch parameterization to all the other Yukawa matrices including the leptons[17]. This results in the ansatz as in Eq.(8) with all ξ_{ij} being of the same order of magnitude. It is not difficult to see that such an ansatz seems conflict with the current experiment data in the lepton sector. This is because in order to explain the most

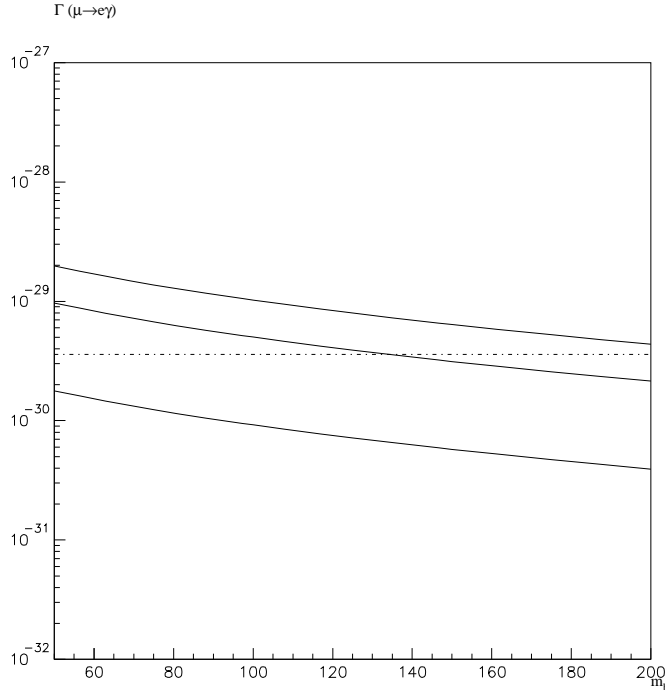


FIG. 8: Contribution to decay $\mu \rightarrow e\gamma$ from the two loop flavour changing Barr-Zee diagrams. The three solid curves (from down to up) correspond to $Y_{\mu e} = 3 \times 10^{-6}, 7 \times 10^{-6}$ and 1×10^{-5} respectively. The horizontal line indicates the experimental upper bound of $\mu \rightarrow e\gamma$

recent data on muon $g - 2$, some off-diagonal elements of the Yukawa coupling matrices should be large, while to meet the constraints from $\mu \rightarrow e\gamma$, some other elements should be greatly suppressed. In the case of muon $g - 2$, If the flavor-conserving Barr-Zee Diagram is playing the major role, the rescaled coupling ξ_μ should be as large as 50 (for one loop flavor conserving contribution, ξ_μ should be even larger). If one assumes that the flavor-changing coupling is responsible for the large muon $g - 2$, $\xi_{\mu\tau}$ should be about 10. On the other hand, due to the strong constraint from $\mu \rightarrow e\gamma$, for the flavor-changing contribution dominated case, $\xi_{\tau e}$ has to be less than 0.08 when $Y_{\mu\tau} = 0.03$ and $m_h = 150$ GeV. In the case of flavor changing Barr-Zee diagram dominant, the Yukawa coupling $\xi_{\mu e}$ has to be less than 0.24 at $m_h = 150$ GeV. Thus the rescaled couplings ξ_{ij} are not in the same order of magnitude. In light of the recent data, it seems that the Yukawa matrix should have a texture different from the one given in Eq.(8). The off-diagonal elements associated with the first generation lepton should be further suppressed, while the one associated with the second and third generation leptons could be considerably large.

From the above considerations, it is suggested that the Yukawa matrices associated with the physical scalar bosons may take the following form in the mass eigenstate

$$Y \simeq \lambda^2 \begin{pmatrix} \mathcal{O}(1) & \mathcal{O}(\lambda^3) & \mathcal{O}(\lambda^3) \\ \mathcal{O}(\lambda^3) & \mathcal{O}(1) & \mathcal{O}(1) \\ \mathcal{O}(\lambda^3) & \mathcal{O}(1) & \mathcal{O}(1) \end{pmatrix} \quad (13)$$

where $\lambda \approx 0.22$ is roughly of the same order of the Wolfenstein parameter λ . With such a parameterization, one is able to understand all the current experimental data concerning both muon $g - 2$ and lepton flavor-changing processes.

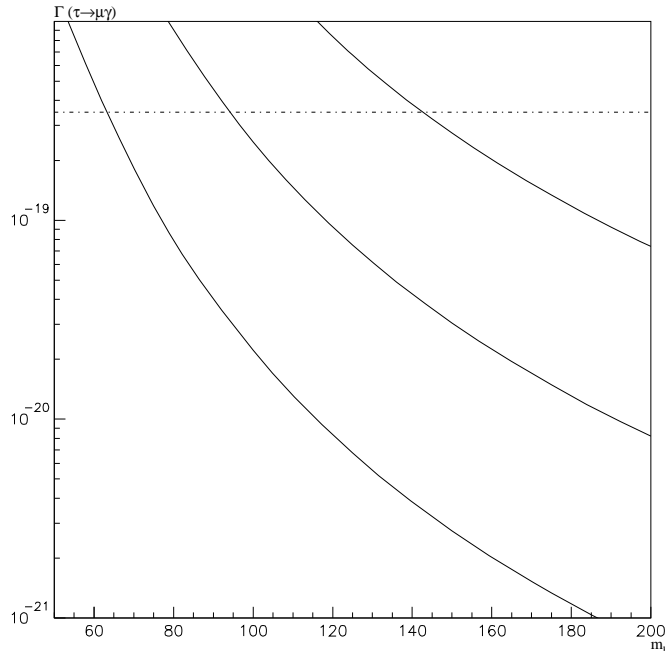


FIG. 9: Prediction of decay rate $\tau \rightarrow \mu\gamma$ from the sum of one loop and two loop double scalar diagrams. The three solid curves (from down to up) correspond to $Y_{\tau\tau}$: 0.003, 0.01 and 0.03 respectively. The coupling $Y_{\mu\tau}$ is taken to be 0.08. The horizontal line indicates the experimental upper bound of $\tau \rightarrow \mu\gamma$

If one takes the Yukawa matrix of the form in Eq.(13), the decay rate of $\tau \rightarrow \mu\gamma$ could be predicted. Assuming τ lepton dominance in the loop, the contribution to $\tau \rightarrow \mu\gamma$ is calculated and shown in Fig.9. The current upper bound on $\tau \rightarrow \mu\gamma$ is 3.5×10^{-19} GeV[26]. It is found that, the predicted decay rate could reach the current experimental bound. A modest improvement in the precision of the present experiment for $\tau \rightarrow \mu\gamma$ may yield a first evidence of lepton family number non-conservation.

In summary, we have studied the muon $g - 2$ and several lepton flavour violation processes in the models with flavour-changing scalar interactions. The two loop diagrams with double scalar exchanges have been investigated and their contribution to muon $g - 2$ is found to be compatible with the one from Barr-Zee diagram. The constraints on Yukawa coupling constants have been resulted from the current data of muon $g - 2$ and several lepton flavour violation processes. The results have shown a very strong constraints on the flavour-changing couplings associated with the first generation lepton. The early ansatz that the flavour changing couplings are proportional to the square root of the products of related fermion masses may not be suitable for the lepton sector. It has been shown that an alternative simple parameterization given in eq.(11) is more attractive to understand the current experimental

data. With such a parameterization, the decay rate of $\tau \rightarrow \mu\gamma$ is found to be close to the current experiment upper bound.

Acknowledgments

This work is supported in part by the Chinese Academy of Sciences and NSFC under Grant # 19625514.

APPENDIX A: TWO LOOP DOUBLE SCALAR DIAGRAMS IN MUON $g - 2$ AND $\mu \rightarrow e\gamma$

From the Yukawa interaction shown in Eq.(3). the $\bar{q}q\phi$ vertex has the following form in d dimension.

$$ig\mu^{\epsilon/2}(Y_1 + Y_2\gamma_5) \quad (\text{A1})$$

where μ is renormalization scale and $\epsilon/2 = 2 - d/2$. The amplitude M for upper loop is given by

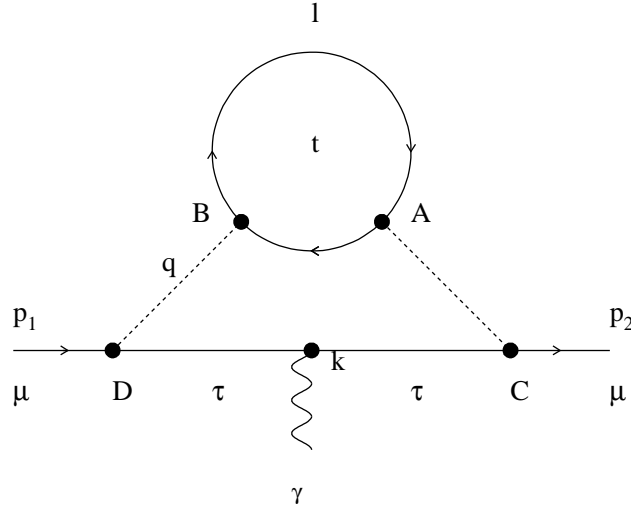


FIG. 10: Two loop double scalar exchanging digram

$$M = -g^2\mu^\epsilon \cdot 2N_C \int \frac{d^d l}{(2\pi)^d} [(A_1 + A_2\gamma_5)(l + \not{k} + m_f)(B_1 + B_2\gamma_5)(l + m_f)] \frac{1}{(l+q)^2 - m_\tau^2} \frac{1}{l^2 - m_f^2} \frac{1}{(A_2)}$$

where N_C and m_f are the color number and mass of fermion f . For t quark $f = t$ and $N_C = 3$. $A_{1,2}$ and $B_{1,2}$ are the couplings of vertex A and B . After Feynman parameterization and momentum integration, we have

$$M = -4 \cdot N_C g^2 \mu^\epsilon (A_1 B_1 - A_2 B_2) \frac{i}{(4\pi)^{2-\epsilon/2}} \Gamma\left(\frac{\epsilon}{2}\right) \int_0^1 dx \left(\left(2 + \frac{\epsilon}{2}\right) [x(x-1)]^{1-\epsilon/2} \frac{1}{(q^2 - R)^{\frac{\epsilon}{2}-1}} + C_{ab} m_f^2 [x(x-1)]^{-\epsilon/2} \frac{1}{(q^2 - R)^{\frac{\epsilon}{2}}} \right) \quad (\text{A3})$$

with $R = m_f^2/[x(1-x)]$ and $C_{ab} = 2A_2 B_2/(A_1 B_1 - A_2 B_2)$. The amplitude for the lower loop is given by

$$I_\mu = -g^2 \mu^\epsilon \bar{\ell}(p_2) (C_1 + C_2 \gamma_5) (\not{p}_2 - \not{q} + m_\tau) \gamma_\mu (\not{p}_1 - \not{q} + m_\tau) (D_1 + D_2 \gamma_5) \ell(p_1) \times \frac{1}{(q-p_2)^2 - m_\tau^2} \cdot \frac{1}{(q-p_1)^2 - m_\tau^2} \cdot \frac{1}{(q^2 - m_\phi^2)^2} \quad (\text{A4})$$

where $C_{1,2}$ and $D_{1,2}$ are the couplings for vertex C and D . Therefore the total amplitude reads

$$\begin{aligned} \Gamma_\mu &= M \cdot I_\mu \\ &= 4 \cdot 2N_C g^4 \mu^{2\epsilon} (A_1 B_1 - A_2 B_2) \frac{i}{(4\pi)^{2-\epsilon/2}} \Gamma\left(\frac{\epsilon}{2}\right) \int_0^1 dx \left(\left(2 + \frac{\epsilon}{2}\right) (x(x-1))^{1-\epsilon/2} \frac{1}{(q^2 - R)^{\epsilon/2-1}} + C_{ab} m_f^2 (x(x-1))^{-\epsilon/2} \frac{1}{(q^2 - R)^{\epsilon/2}} \right) \\ &\quad \cdot 6 \int_0^1 dy \int_0^{1-y} dz (1-y-z) \int \frac{d^d q'}{(2\pi)^d} \frac{1}{(q'^2 - \Delta')^4} \cdot \mathcal{N} \end{aligned} \quad (\text{A5})$$

with $q' = q - yp_2 - zp_1$ and $\Delta' = (y+z)m_\tau^2 + (1-y-z)m_\phi^2$. Where the factor 2 comes from the diagram with C and D are interchanged.

After integrating over q' and isolating the poles from Feynman integration, we obtain

$$\begin{aligned} \Gamma_\mu &= \frac{-8 \cdot 2N_C g^4 (A_1 B_1 - A_2 B_2) m_\tau m_\mu}{(4\pi)^4} \times \int_0^1 dx 2x(1-x) \int_0^1 dy \int_0^{1-y} dz (y+z)(1-y-z) \\ &\quad \left(\left(\left(\frac{2}{\epsilon} - 2\gamma_E + 2 \ln 4\pi - \ln x(1-x) + \frac{1}{2} \right) \cdot f_{1,div} + 2 \cdot f_{1,con} \right) \right. \\ &\quad \left. + \frac{1}{2} C_{ab} R \cdot \left(\left(\frac{2}{\epsilon} - 2\gamma_E + 2 \ln 4\pi - \ln x(1-x) \right) \cdot f_{2,div} + 2 \cdot f_{2,con} \right) \right) \\ &\quad \bar{\ell} (C_1 D_1 + C_2 D_2 + (C_1 D_2 + C_2 D_1) \gamma_5) \frac{i \sigma^{\mu\nu} k_\nu}{2m_\mu} \ell \end{aligned} \quad (\text{A6})$$

with

$$f_{1,div} = \frac{3\Delta' + R}{\Delta'^2}, \quad f_{2,div} = -\frac{1}{\Delta'^2} \quad (\text{A7})$$

and,

$$f_{1,con} = \left\{ -13\Delta'^4 + 38\Delta'^3 R - 37\Delta'^2 R^2 + 14\Delta' R^3 - 2R^4 \right.$$

$$\begin{aligned}
& +(-12\Delta'^4 + 32\Delta'^3 R - 24\Delta'^2 R^2) \ln\left(\frac{R}{\mu^2}\right) + 4R^4 \ln\left(\frac{\Delta'}{\mu^2}\right) \\
& +(-2\Delta'^4 + 32\Delta'^3 R - 24\Delta'^2 R^2 - 2R^4) \ln\left(\frac{\Delta'}{R}\right) \left. \vphantom{\frac{1}{4\Delta'^2(\Delta' - R)^3}} \right\} \frac{1}{4\Delta'^2(\Delta' - R)^3} \\
f_{2,con} = & \left\{ 3\Delta'^4 - 10\Delta'^3 R + 7\Delta'^2 R^2 - 2\Delta' R^3 + 2R^4 \right. \\
& + 4R^3(R - 4\Delta') \ln\frac{\Delta'}{\mu^2} + 2(2\Delta'^4 - 8\Delta'^3 R + 12\Delta'^2 R^2 + 4\Delta' R^3 - R^4) \ln\frac{\Delta'}{R} \\
& \left. 4(\Delta'^4 - 4\Delta'^3 R + 6\Delta'^2 R^2) \ln\frac{R}{\mu^2} \right\} \frac{1}{4\Delta'^2(\Delta' - R)^4} \tag{A8}
\end{aligned}$$

In large m_f limit, i.e. $m_f^2 \gg \frac{1}{4}m_\phi^2 \gg m_\tau^2$, one has

$$\begin{aligned}
f_{1,div} & \rightarrow \frac{R}{\Delta'^2}, & f_{2,div} & \rightarrow -\frac{1}{\Delta'^2} \\
f_{1,con} & \rightarrow \frac{R}{2\Delta'^2} \left[1 - \ln\left(\frac{\Delta' R}{\mu^4}\right) \right], & f_{2,con} & \rightarrow \frac{1}{2\Delta'^2} \left[1 + \ln\frac{\Delta' R}{\mu^4} \right] \tag{A9}
\end{aligned}$$

The counter term of upper loop has the following form

$$C = i(\delta Z q^2 - \delta m_\phi^2) \tag{A10}$$

With δZ and δm^2 are the wave function and mass renormalization constants respectively. In the On-Shell Renormalization scheme, they are given by

$$\begin{aligned}
\delta Z & = -4 \cdot 2N_C g^2 (A_1 B_1 - A_2 B_2) \frac{1}{(4\pi)^2} \int_0^1 dx \cdot 2x(1-x) \left(\frac{2}{\epsilon} - \gamma_E + \ln 4\pi + \frac{1}{2} - \mathcal{F}(x) \right) \\
\delta m_\phi^2 & = -4 \cdot 2N_C g^2 (A_1 B_1 - A_2 B_2) \frac{1}{(4\pi)^2} \int_0^1 dx m_f^2 \\
& \left\{ 2 \cdot \left(\frac{2}{\epsilon} - \gamma_E + \ln 4\pi + \frac{1}{2} - \mathcal{F}(x) \right) + C_{ab} \left(\frac{2}{\epsilon} - \gamma_E + \ln 4\pi - \mathcal{F}(x) \right) \right\} \tag{A11}
\end{aligned}$$

with

$$\mathcal{F}(x) = \left(\ln \frac{m_f^2 - x(1-x)m_\phi^2}{\mu^2} \right) \tag{A12}$$

Inserting the counter terms to the lower loop, the counter term at two loop level is given by

$$\begin{aligned}
\delta \Gamma_\mu & = \bar{\ell}(p_2) i g \mu^{\epsilon/2} (C_1 + C_2 \gamma_5) \frac{i}{\not{p}_2 - \not{q} - m_\tau} \gamma_\mu \frac{i}{\not{p}_1 - \not{q} - m_\tau} \\
& i g \mu^{\epsilon/2} (D_1 + D_2 \gamma_5) \ell(p_1) \frac{i}{q^2 - m_\phi^2} \cdot \frac{i}{q^2 - m_\phi^2} \cdot i(\delta Z q^2 - \delta m_\phi^2) \\
& = -i g^2 \mu^\epsilon \cdot 6 \int_0^1 dy \int_0^{1-y} dz (1-y-z) \frac{1}{(q'^2 - \Delta')^4} \mathcal{N} \tag{A13}
\end{aligned}$$

with

$$\mathcal{N} = 2(y+z)m_\tau m_\mu \bar{\ell}(p_2) (C_1 D_1 + C_2 D_2 + (C_1 D_2 + C_2 D_1) \gamma_5) \left[\left(1 + \frac{1}{2} \left(1 + \frac{\epsilon}{4} \right) \delta Z q'^2 - \delta m_\phi^2 \right) \frac{i \sigma_{\mu\nu} k^\nu}{2m_\mu} \ell(p_1) \right] \tag{A14}$$

after integration over q' , we arrive at

$$\begin{aligned} \delta\Gamma_\mu &= \frac{-8 \cdot 2N_C g^4 m_\tau m_\mu (A_1 B_1 - A_2 B_2)}{(4\pi)^4} \int_0^1 dx \, 2x(1-x) \int_0^1 dy \int_0^{1-y} dz \, (y+z)(1-y-z) \\ &\quad \left\{ \bar{\ell}(p_2) (C_1 D_1 + C_2 D_2 + (C_1 D_2 + C_2 D_1) \gamma_5) \left[-\frac{3\Delta' + R}{\Delta'^2} \left(\frac{2}{\epsilon} - 2\gamma_E + 2 \ln 4\pi - \mathcal{F}(x) - \ln \frac{\Delta'}{\mu^2} \right) \right. \right. \\ &\quad \left. \left. + \frac{3}{2\Delta'} - \frac{R}{\Delta'^2} + \frac{1}{\Delta'^2} \frac{1}{2} C_{ab} R \left(\frac{2}{\epsilon} - 2\gamma_E + 2 \ln 4\pi - \mathcal{F}(x) - \ln \frac{\Delta'}{\mu^2} \right) \right] \frac{i\sigma_{\mu\nu} k^\nu}{2m_\mu} \ell(p_1) \right\} \end{aligned} \quad (\text{A15})$$

Adding the counter term into the amplitude, the ultraviolet divergences are canceled. The physical amplitude is given by

$$\begin{aligned} \Gamma_\mu^B &= \Gamma_\mu + \delta\Gamma_\mu \\ &= \frac{-8 \cdot 2N_C g^4 m_\tau m_\mu (A_1 B_1 - A_2 B_2)}{(4\pi)^4} \int_0^1 dx \, 2x(1-x) \int_0^1 dy \int_0^{1-y} dz \, (y+z)(1-y-z) \\ &\quad \left[+\frac{3\Delta' + R}{\Delta'^2} \left(-\ln x(1-x) + \frac{1}{2} + \mathcal{F}(x) + \ln \frac{\Delta'}{\mu^2} \right) + 2 \cdot f_{1,con} \right. \\ &\quad \left. -\frac{1}{\Delta'^2} \frac{1}{2} C_{ab} R \left(-\ln x(1-x) + \frac{1}{2} + \mathcal{F}(x) + \ln \frac{\Delta'}{\mu^2} \right) + \frac{1}{2} C_{ab} R \left(2 \cdot f_{2,con} - \frac{1}{2} \right) + \frac{3\Delta' - 2R}{2\Delta'^2} \right] \\ &\quad \bar{\ell}(p_2) (C_1 D_1 + C_2 D_2 + (C_1 D_2 + C_2 D_1) \gamma_5) \frac{i\sigma_{\mu\nu} k^\nu}{2m_\mu} \ell(p_1) \end{aligned} \quad (\text{A16})$$

with

$$\mathcal{F}(x) = \ln \frac{m_f^2 - x(1-x)m_\tau^2}{\mu^2} \quad (\text{A17})$$

In the limit of $m_f^2 \gg \frac{1}{4}m_\phi^2 \gg m_\tau^2$, The above equation can be simplified as

$$\begin{aligned} \Gamma_\mu^B &= -\frac{N_C g^4 m_\tau m_\mu m_f^2 (A_1 B_1 + A_2 B_2)}{16\pi^4 m_\phi^4} \left(-\frac{5}{2} + \ln \frac{m_\phi^2}{m_\tau^2} \right) \\ &\quad \left((C_1 D_1 + C_2 D_2) \bar{\ell}(p_2) \frac{i\sigma_{\mu\nu} k^\nu}{2m_\mu} \ell(p_1) + (C_1 D_2 + C_2 D_1) \bar{\ell}(p_2) \frac{i\sigma_{\mu\nu} k^\nu \gamma_5}{2m_\mu} \ell(p_1) \right) \end{aligned} \quad (\text{A18})$$

Hence in the $\mu \rightarrow \mu\gamma$ transition, its contribution to muon $g-2$ is

$$\Delta a_\mu = -\frac{N_C g^4 m_\tau m_\mu m_f^2}{16\pi^4 m_\phi^4} \left(-\frac{5}{2} + \ln \frac{m_\phi^2}{m_\tau^2} \right) (A_1 B_1 + A_2 B_2) (C_1 D_1 + C_2 D_2) \quad (\text{A19})$$

Similarly, in the $\mu \rightarrow e\gamma$ transition, its contribution to $\Gamma(\mu \rightarrow e\gamma)$ is

$$\Gamma(\mu \rightarrow e\gamma) = \frac{m_\mu^3}{8\pi} \left[\frac{N_C g^4 m_\tau m_f^2}{32\pi^4 m_\phi^4} \left(-\frac{5}{2} + \ln \frac{m_\phi^2}{m_\tau^2} \right) \right]^2 |(A_1 B_1 + A_2 B_2)|^2 \cdot (|C'_1 D_1 + C'_2 D_2|^2 + |C'_1 D_2 + C'_2 D_1|^2) \quad (\text{A20})$$

For scalar exchange, taking

$$A_1 = B_1 = Y_{ff}, \quad C_1 = D_1 = Y_{\mu\tau} \quad (\text{A21})$$

and others are zero. For pseudoscalar exchange

$$A_2 = B_2 = iY_{ff}, \quad C_2 = D_2 = iY_{\mu\tau} \quad (\text{A22})$$

Therefore, the two loop double scalar (pseudo-scalar) diagram's contribution to Δa_μ is

$$\Delta a_\mu = \mp \frac{N_C g^4 m_\tau m_\mu m_f^2}{16\pi^4 m_\phi^4} \left(-\frac{5}{2} + \ln \frac{m_\phi^2}{m_\tau^2} \right) Y_{tt}^2 Y_{\mu\tau}^2 \quad (\text{A23})$$

- [1] H. N. Brown et al. (Muon g-2), Phys. Rev. Lett. **86**, 2227 (2001), hep-ex/0102017.
- [2] S. J. Brodsky and J. D. Sullivan, Phys. Rev. **D156**, 1644 (1967), T. Burnett and M. J. Levine, Phys. Lett. **B24**, 467 (1967), M. Gourdin and E. de Rafael, Nucl. Phys. **B10**, 667 (1969), R. Jackiw and S. Weinberg, Phys. Rev. **D5**, 2473 (1972), K. Fujikawa, B. W. Lee, and A. I. Sanda, Phys. Rev. **D6**, 2923 (1972), I. Bars and M. Yoshimura, Phys. Rev. **D6**, 374 (1972), G. Altarelli, N. Cabibbo, and L. Maiani, Phys. Lett. **B40**, 415 (1972), W. A. Bardeen, R. Gastmans, and B. E. Lautrup, Nucl. Phys. **B46**, 315(1972), A. Czarnecki, B. Krause and W. Marciano, Phys. Rev. **D52**, R2619 (1995), S. Peris, M. Perrottet, and E. de Rafael, Phys. Lett. **B355**, 523 (1995), A. Czarnecki, B. Krause and W. Marciano, Phys. Lett. **B76**, 3267 (1996), G. Degrossi and G. F. Giudice, Phys. Rev. **D58**, 053007 (1998), M. Davier and A. Höcker, Phys. Lett. **B435**, 427 (1998), M. Davier, Nucl. Phys. B (Proc. Suppl.) **76**, 327 (1999).
- [3] See for example, U. Chattopadhyay, D. K. Ghosh, S. Roy, hep-ph/0006049; L. Everett, G. L. Kane, S. Rigolin, L. T. Wang, hep-ph/0102145; J. L. Feng, K. T. Matchev, hep-ph/0102146; U. Chattopadhyay, P. Nath, hep-ph/0102157; S. Komine, T. Moroi, M. Yamaguchi, hep-ph/0102204; J. Hisano, K. Tobe, hep-ph/0102315; J. E. Kim, B. Kyae, H. M. Lee, hep-ph/0103054; S. P. Martin, J. D. Wells, hep-ph/0103067; H. Baer, C. Balazs, J. Ferrandis, X. Tata, hep-ph/0103280; G. C. McLaughlin, J. N. Ng, hep-ph/0008209; S. C. Park, H. S. Song, hep-ph/0103072; C. S. Kim, J. D. Kim, J. Song, hep-ph/0103127; K. Agashe, N.G. Deshpande, G.-H. Wu, hep-ph/0103235; K. Choi, et. al, hep-ph/0103048; E. Ma and M. Raidal, hep-ph/0102255; R. Arnowitt, B. Dutta, B. Hu and Y. Santoso, hep-ph/0102344; V. Barger, et. al, hep-ph/0101106 R. Casadio, A. Gruppuso and G. Venturi, hep-th/0010065; C.H. Chen and C.Q. Geng, hep-ph/0104151.
- [4] Y.-L. Wu and Y.-F. Zhou (2001), hep-ph/0104056, to appear in Phys. Rev. **D**.
- [5] M. Raidal, Phys. Lett. **B508**, 51 (2001), arXiv:hep-ph/0103224.
- [6] Y.L. Wu and L. Wolfenstein, Phys. Rev. Lett. **73**, 1762 (1994). L. Wolfenstein and Y.L. Wu, Phys. Rev. Lett., **73**, 2809(1994). For more detailed analyses, see: Y.L. Wu, Carnegie-Mellon Report, hep-ph/9404241, 1994 (unpublished); *A Model for the Origin and Mechanisms of CP Violation*, in: Proceedings at 5th Conference on the Intersections of Particle and Nuclear Physics, St. Petersburg, FL, 31 May- 6 Jun 1994, pp338, edited by S.J. Seestrom (AIP, New York, 1995).
- [7] T. D. Lee, Phys. Rev. **D8**, 1226 (1973).
- [8] T. D. Lee, Phys. Rept. **9**, 143 (1974).
- [9] P. Sikivie, Phys. Lett. **B65**, 141 (1976); H.E. Haber, G.L. Kane and T. Sterling, Nucl. Phys. **B161**, 493 (1979); N.G. Deshpande and E. Ma, Phys. rev. **D18**, 2574 (1978); H. Georgi, Hadronic J. **1**, 155 (1978); J.F. Donoghue and L.-F. Li, Phys. Rev. **D19**, 945 (1979); A.B.

- Lahanas and C.E. Vayonakis, Phys. Rev. **D19**, 2158 (1979); L.F. Abbott, P. Sikivie and M.B. Wise, Phys. Rev. **D21**, 1393 (1980); G.C. Branco, A.J. Buras and J.M. Gerard, Nucl. Phys. **B259**, 306 (1985); B. McWilliams and L.-F. Li, Nucl. Phys. **B179**, 62 (1981); J.F. Gunion and H.E. Haber, Nucl. Phys. **B272**, 1 (1986); J. Liu and L. Wolfenstein, Nucl. Phys. **B289**, 1 (1987).
- [10] A. Dedes and H. E. Haber (2001), hep-ph/0105014.
- [11] A. Dedes and H. E. Haber, JHEP **05**, 006 (2001), hep-ph/0102297.
- [12] M. Krawczyk (2001), hep-ph/0103223.
- [13] J. R. Primack and H.R. Quinn, Phys. Rev. **D6**, 3171 (1972); W. A. Bardeen, R. Gastmans and B. Lautrup, Nucl. Phys. B **46**, 319 (1972); J. P. Leveille, Nucl. Phys. B **137**, 63 (1978); H. E. Haber, G. L. Kane and T. Sterling, Nucl. Phys. B **161**, 493 (1979); E. D. Carlson, S.L. Glashow and U. Sarid, Nucl. Phys. B **309**, 597 (1988);.
- [14] J. D. Bjorken and S. Weinberg. Phys. Rev. Lett. **38** , 622 (1977), S. M. Barr and A. Zee, Phys. Rev. Lett. **65** , 21 (1990).
- [15] D. Chang, W.-F. Chang, C.-H. Chou, and W.-Y. Keung, Phys. Rev. **D63**, 091301 (2001), hep-ph/0009292.
- [16] K. Cheung, C.-H. Chou, and O. C. W. Kong (2001), hep-ph/0103183.
- [17] T. P. Cheng and M. Sher, Phys. Rev. **D35**, 3484 (1987).
- [18] M. Sher and Y. Yuan, Phys. Rev. **D44**, 1461 (1991).
- [19] D. Atwood, L. Reina, and A. Soni, Phys. Rev. Lett. **75**, 3800 (1995), hep-ph/9507416.
- [20] D. Atwood, L. Reina, and A. Soni, Phys. Rev. **D55**, 3156 (1997), hep-ph/9609279.
- [21] Y. L. Wu and Y. F. Zhou, Phys. Rev. **D61**, 096001 (2000), hep-ph/9906313.
- [22] M. Sher, Phys. Lett. **B487**, 151 (2000), hep-ph/0006159.
- [23] S. Nie and M. Sher, Phys. Rev. **D58**, 097701 (1998), hep-ph/9805376.
- [24] S. K. Kang and K. Y. Lee (2001), hep-ph/0103064.
- [25] R. Diaz, R. Martinez, and J. A. Rodriguez (2000), hep-ph/0010149.
- [26] D. E. Groom et al. (Particle Data Group), EPJ. **C15**, 1 (2000).
- [27] H. Fritzsch, Nucl. Phys. **B155**, 189 (1979).